Effects of Substituent and Leaving Group on the Gas-Phase S_N2 Reactions of Phenoxides with Halomethanes: A DFT Investigation

Qiang-gen Li[†] and Ying Xue*[,†,‡]

College of Chemistry, Key Lab of Green Chemistry and Technology in Ministry of Education, Sichuan University, Chengdu, 610064, People's Republic of China, and State Key Laboratory of Biotherapy, Sichuan University, Chengdu 610041, P. R. China

Received: June 7, 2009; Revised Manuscript Received: July 25, 2009

Computational investigations on the gas-phase nucleophilic substitution reactions of *p*-substituted phenoxides (*p*-Y-$C_6H_4O^-$, Y = OH, CH_3O, CH_3, H, F, Cl, CF_3) with halomethanes (CH_3X, X = F, Cl, Br, and I) were performed by the B3LYP and MP2 methods with the 6-311+G(d,p) basis set. Calculated results indicate that the reactions are more endothermic only when the substrate is a lighter halide. The complexation enthalpies, the key parameters in the transition state (TS), the central barriers, overall barriers, overall reaction enthalpies, and the charge of the O4 atom in the TSs all present good correlations with the Hammett constants σ of substituents in the nucleophile. Leffler−Grunwald rate equilibrium relationships predict the degree of bond formation in the transition state suggesting that the reactions have progressed 31%, 24%, 24%, and 21% in the TS for halomethanes (X = F, Cl, Br, and I), respectively. The TS structure with substituents in the nucleophile is not kinetically but thermodynamically controlled, similar to the earlier results. Furthermore, the excellent relationship between the central barrier heights and the looseness of the transition state structure indicates that the stretching of the cleaving bond is one of the major factors determining the central barrier heights. The nucleophilicity of the nucleophile decreases with the increase of the electron-withdrawing power of substituent Y in the nucleophile, while the leaving-group ability of the halogen atom increases with the decrease of its Mulliken electronegativity.

1. Introduction

Bimolecular nucleophilic substitution (S_N2) reactions are of great importance for both chemical[1,2] and biochemical processes,[3] and their mechanisms are well established from numerous experimental kinetic and theoretical studies.[4−20] In the past decades, much attention had focused on the effects of structural variations in both substrate and nucleophile on such a reaction process. Especially in the latest decade, many continuing studies were seen on the relationships between structure and reactivity for S_N2 reactions. Some reviews[21−23] are particularly relevant. Brauman et al.[24,25] studied the steric retardation of S_N2 reactions of some alkyl chlorides as well as α-cyanoalkyl derivatives in the gas phase and solution through experimental and theoretical investigations, discovering that the activation energies for S_N2 reactions vary with steric effects both in the gas phase and in polar solvents. Ren and Yamataka[26−28] used G2(+) theory to re-examine the gas-phase S_N2 reactions at saturated carbon for model reactions, finding that the α-effect exists in the gas phase, and its size varies depending on the R group of the substrate and the identity of the α-atom of the nucleophile. Galabov et al.[29] applied ab initio methods and carefully calibrated density functional theory to the S_N2 identity exchange reactions of fluoride ion with benzyl fluoride and 10 para-substituted derivatives. They disclosed the origin of the S_N2 benzylic effect and concluded that the S_N2 reactivity of their studied benzylic compounds is governed by the intrinsic electrostatic interaction between the reacting fragments. Bento and Bickelhaupt[30] very recently used the density functional theory (DFT) at the ZORA-OLYP/TZ2P level to study the backside and front side S_N2 reactions at saturated carbon. Their results indicated that the nucleophilicity is determined by the electron-donor capability of the nucleophile, and leaving-group ability derives directly from carbon leaving group bond strength. For the effect of substituents on the S_N2 reaction, most of the studies have been on the effects of structural variations in substrate[29,31−41] and relatively less on the nucleophile.[42−47]

Phenoxide is one of the ordinary nucleophiles in the chemical process. Its reactivity is strongly affected by the delocalization of an electron pair from oxygen onto the aromatic ring, which causes a decrease in the basicity of the phenol oxygen further decreasing its nucleophilic ability. The substituent of the aromatic ring will dominate the degree of delocalization of an electron pair from oxygen onto the aromatic ring. In 1998, Kim et al.[42] investigated the gas-phase substituent effects in S_N2 reactions of benzyl chloride derivatives with phenoxides and thiophenoxides using the PM3 semiempirical molecular orbital method. They found that the degree of bond formation in the transition state (TS) is approximately 45% and 40% on the reaction coordinate for the phenoxides and thiophenoxides, respectively. The weaker nucleophile of thiophenoxides leads to a later TS with an increased bond making and breaking. Furthermore, variation of the TS structure with substituents in the nucleophile is thermodynamically controlled and is well correlated by Leffler−Grunwald rate-equilibrium relationships. Although they did a perfect work, they did not consider the effects of electron-donating substituents in the nucleophile on the reactions. Moreover, for the sake of reducing the compu-

* Corresponding author. E-mail address: yxue@scu.edu.cn. Tel.: 86-28-85418330.
[†] College of Chemistry.
[‡] State Key Laboratory of Biotherapy.

10.1021/jp905346e CCC: $40.75
Published on Web 08/27/2009

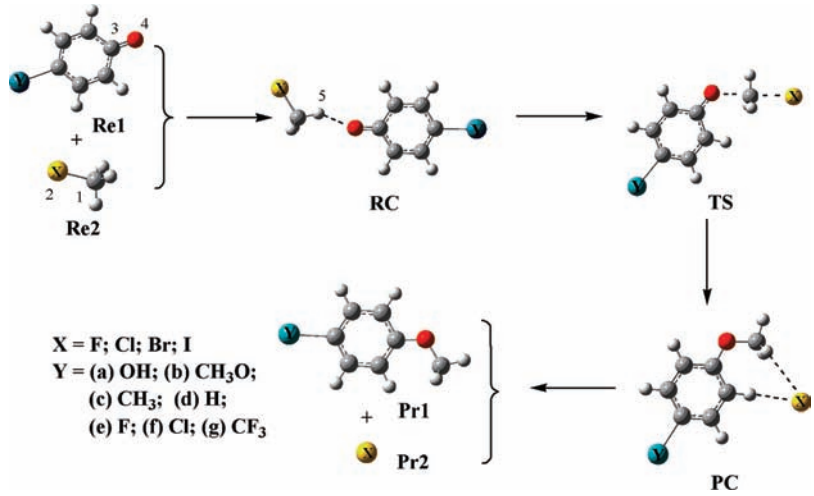

Figure 1. Reaction pathway of the S_N2 nucleophilic substitution reactions $YC_6H_4O^- + CH_3X$ (X = F, Cl, Br, I; Y = OH, CH_3O, CH_3, H, F, Cl, CF_3).

tational cost, they used the lower level of theory of the PM3 semiempirical MO method in their study.

The fast development of the computer capability enables us to deal with the larger chemical system by a higher level of theory. To enrich the theoretical study on the effects of structural variations in the nucleophile on the S_N2 reaction, in this work, we used the density functional theory B3LYP/6-311+G(d,p) method to investigate the gas-phase nucleophilic substitution reactions of *p*-substituted phenoxides (*p*-Y-$C_6H_4O^-$, Y = OH, CH_3O, CH_3, H, F, Cl, and CF_3) with halomethanes (CH_3X, X = F, Cl, Br, and I) (see Figure 1). More attention will focus on the effects of substituent and leaving group on the reaction barriers, the structures of transition state, and the natural charge distributions. Meanwhile, we will discus the nucleophilicity of the nucleophile and leaving-group ability of the halogen atom in the substrate. The results will be compared with those in the earlier studies.[30,42] We hope to provide some useful information for the further experimental or theoretical studies.

2. Computational Details

The geometric optimization of all species in this study was carried out using the density functional theory (DFT) with Becke's three-parameter (B3)[48] exchange functional along with the Lee−Yang−Parr (LYP) nonlocal correlation functional (B3LYP).[49,50] The DFT approach was chosen in this study due to its partial inclusion of electron correlation effect, which is expected to give a much better description of reaction barriers and hydrogen bonds than the Hartree−Fock method. In addition, the DFT(B3LYP) approach has recently been successfully applied to study the substituent effect on the S_N2 reaction.[29,38−41,45,47] In this work, all the geometries of the stationary points, including the separated reactant (**Re1** and **Re2**), reactant complex (**RC**), the transition state (**TS**), the product complex (**PC**), and the separated product (**Pr1** and **Pr2**), were fully optimized without symmetry constraints at the B3LYP/6-311+G(d,p) level of theory. The nature of all optimized structures was determined by calculating the harmonic vibrational frequencies, with the use of analytical second derivatives. No or one imaginary frequency was obtained for true minima and transition states, respectively. The frequency calculations at the B3LYP/6-311+G(d,p) level without scaling also provided thermodynamic quantities such as the zero-point vibrational energy, thermal correction, enthalpies, Gibbs free energies, and entropies at 298.15 K and 1.0 atm. Single-point MP2 calculations, MP2/6-311+G(d,p)//B3LYP/6-311+G(d,p), were also carried out to assess the accuracy of the B3LYP energies.

All electron (AE) calculations were run for the fluorine-, chlorine-, and oxygen-containing species, while Wadt and Hay[51] effective core potentials (ECP) were used for bromine- and iodine-containing species. Charge distributions were obtained employing natural population analysis (NPA)[52,53] from the wave functions calculated at the MP2/6-311+G(d,p)//B3LYP/6-311+G(d,p) level.

Throughout this study, all calculations were performed using the Gaussian 03 program.[54] All internuclear distances are in angstroms, and all angles are in degrees. The relative energy in the gas phase (denoted as ΔH in kcal/mol) is computed using the enthalpy value at 298.15 K and 1 atm, which is obtained by adding the enthalpy correction at the B3LYP/6-311+G(d,p) level to the electronic energy at the MP2/6-311+G(d,p)//B3LYP/6-311+G(d,p) level.

3. Results and Discussions

It is well-known that the regular backside-attack S_N2 reaction at C, which goes with inversion of configuration, has a lower reaction barrier than the corresponding frontside pathway, which goes with retention of configuration, mainly because of the increasing steric repulsion between nucleophile and leaving group in the latter transition state.[30] Therefore, only the inversion pathway is considered in this study.

The gas-phase reaction energy profile for the concerted S_N2 reactions of phenoxides with halomethanes is described by an asymmetrical double-well curve (see Scheme 1). The reaction involves the initial formation of a loosely bound reactant ion−molecule complex (**RC**), by the hydrogen bond(s) between phenol oxygen and the hydrogen of halomethane. This ion−molecule complex must then overcome the central barrier ($\Delta H^{\ddagger}$) to reach an asymmetrical linear transition state (**TS**). The latter then breaks down to give the product ion−molecule complex (**PC**), accompanying the formation of the C1−O4 bond and cleavage of the C1−X2 bond. Subsequently, the product ion−molecule complex dissociates into the separate products (**Pr**).

The relative energy data of all the reactions considered in this study are summarized in Table 1. It is interesting that the entropy change values ($\Delta S^{\ddagger}$) of the TSs relative to the reactants for all substituted reaction systems are in a very small range of −30.2∼−37.2 cal·K^{-1}·mol^{-1}. Clearly, the TSs are highly

SCHEME 1: Schematic Potential Energy Profile for the S_N2 Nucleophilic Substitution Reactions $YC_6H_4O^- + CH_3X$ (X = F, Cl, Br, I; Y = OH, CH_3O, CH_3, H, F, Cl, CF_3)

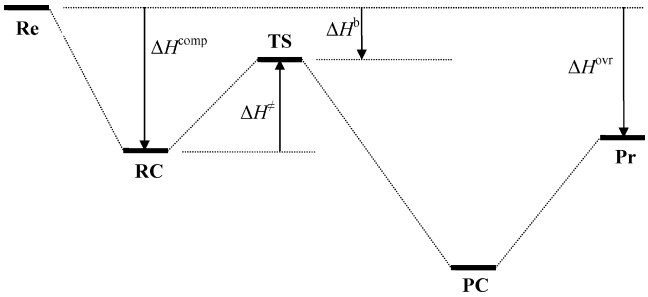

TABLE 1: MP2 Complexation Enthalpies (ΔH^{comp}, kcal/mol), Central Barrier Heights ($\Delta H^{\ddagger}$, kcal/mol), Overall Barrier Height (ΔH^{b}, kcal/mol), Overall Reaction Enthalpies (ΔH^{ovr}, kcal/mol), and the Entropy Changes of the TSs Relative the Reactants ($\Delta S^{\ddagger}$, cal/mol/K) for Reactions $YC_6H_4O^- + CH_3X$ (X = F, Cl, Br, I; Y = OH, CH_3O, CH_3, H, F, Cl, CF_3)

X	Y	ΔH^{comp}	$\Delta H^{\ddagger}$	ΔH^{b}	ΔH^{ovr}	$\Delta S^{\ddagger}$
F	*p*-OH	−6.5	19.6	13.1	18.8	−36.9
	p-CH_3O	−6.4	20.0	13.5	18.5	−38.4
	p-CH_3	−6.3	20.2	13.9	19.4	−35.5
	−H	−6.3	20.5	14.2	20.7	−36.3
	p-F	−6.2	21.0	14.9	23.8	−36.3
	p-Cl	−5.8	22.3	16.4	27.2	−36.4
	p-CF_3	−5.2	24.9	19.6	34.5	−36.2
Cl	*p*-OH	−7.4	6.8	−0.6	−14.6	−34.6
	p-CH_3O	−7.3	7.1	−0.2	−14.9	−35.9
	p-CH_3	−7.2	7.2	0.0	−13.9	−33.9
	−H	−7.1	7.4	0.2	−12.6	−34.2
	p-F	−6.9	7.9	0.9	−9.6	−34.3
	p-Cl	−6.5	8.8	2.3	−6.2	−34.7
	p-CF_3	−5.8	10.9	5.1	1.2	−34.6
Br	*p*-OH	−11.3	3.5	−7.7	−21.6	−37.2
	p-CH_3O	−11.4	4.4	−7.1	−21.9	−35.4
	p-CH_3	−10.9	4.4	−6.4	−20.9	−33.6
	−H	−10.5	4.6	−5.9	−19.7	−33.1
	p-F	−11.0	5.2	−5.8	−16.6	−33.7
	p-Cl	−10.3	6.1	−4.2	−13.2	−34.3
	p-CF_3	−11.3	8.0	−3.4	−5.8	−34.1
I	*p*-OH	−11.4	2.5	−8.9	−27.4	−30.2
	p-CH_3O	−11.6	2.7	−8.9	−27.6	−35.0
	p-CH_3	−11.0	2.8	−8.3	−26.7	−32.6
	−H	−10.7	2.9	−7.8	−25.4	−32.6
	p-F	−11.4	3.4	−7.6	−22.3	−33.2
	p-Cl	−10.3	4.3	−6.1	−18.9	−33.6
	p-CF_3	−11.3	6.1	−5.2	−11.6	−34.6

structured in all the reactions. Hence, the relative enthalpy change is adopted in this study without considering the contribution of the entropy.

3.1. Substrates and Reactant Ion−molecule Complexes. The geometrical parameters for substrates CH_3X (X = F, Cl, Br, and I) are listed in Table 2. The calculated C−X and C−H bond lengths here are very close to the previous results of G2(+) theory[55] and experiments.[56−59] Comparing with the experimental data, the largest deviation for the C−X and C−H bond lengths in CH_3X is 0.035 Å (X = Br) and 0.006 Å (X = F), respectively. Furthermore, the X−C−H angles deviate from the experimental values only by up to 1.0° (X = I), indicating that the computational methods employed in this study are reliable.

When two reactants (**Re1** and **Re2**) are close to each other, a loosely bound reactant ion−molecule complex (**RC**) is formed

TABLE 2: Geometries and Dipole Moments for CH_3X (X = F, Cl, Br, and I)

CH_3X	level	R(C−X)	R(C−H)	∠X−C−H	μ (D)
CH_3F	DFT[a]	1.396	1.092	108.6	2.085
	G2(+)[b]	1.407	1.090	108.0	
	exptl	1.383[c]	1.086[c]	108.8[c]	1.858[g]
CH_3Cl	DFT	1.806	1.087	108.3	2.106
	G2(+)	1.780	1.089	108.9	
	exptl	1.785[d]	1.090[d]	108.1[d]	1.892[g]
CH_3Br	DFT-ECP	1.969	1.086	107.7	2.026
	G2(+)-ECP	1.954	1.088	108.0	
	exptl	1.934[e]	1.082[e]	107.7[e]	1.822[g]
CH_3I	DFT-ECP	2.159	1.085	107.6	1.793
	G2(+)-ECP	2.140	1.088	108.0	
	exptl	2.132[f]	1.085[f]	108.6[f]	1.620[g]

[a] At the B3LYP/6-311+G(d,p) level. [b] At the MP2(fc)/6-31+G(d), from ref 55. [c] Ref 56. [d] Ref 57. [e] Ref 58. [f] Ref 59. [g] Ref 60.

by the hydrogen bond(s) between phenol oxygen and the hydrogen of halomethane. From Table 3, we can see that the O4···H5 hydrogen bond length is sensitive to variations of substituents both in nucleophile and in substrate; i.e., it decreases with the decrease of electronegativity of X in substrate and increases with the strength of the electron-withdrawing power of Y in the nucleophile. For example, when X = Cl, the O4···H5 hydrogen bond lengths vary from 2.012 to 2.086 Å as Y is varied from OH to CF_3. If we fix Y (Y = H) and change the substrate CH_3X going from X = F to I, the O4···H5 hydrogen bond lengths vary from 2.520 to 1.972 Å. This can be explained by the electrostatic interactions between phenol oxygen and the hydrogen of halomethane. The natural population analysis (NPA) shows that the positive charge of the hydrogen atom in CH_3X increases in the order: 0.138 e (X = F) < 0.188 e (X = Cl) < 0.198 e (X = Br) < 0.203 e (X = I). On the other hand, the negative charge of the O4 atom in **Re1** presents a decreasing tendency as the electron-withdrawing power of the substituent Y increases from OH to CF_3.

3.2. Transition State Structures and Barrier Heights. B3LYP/6-311+G(d,p) geometries of the transition state are found to present a linear conformation on the O4···C1···X2 moiety. The key parameters for describing the transition state are the distances of O4···C1 and C1···X2 (see Table 3). The data in Table 3 indicate that the C1−O4 single bond length increases in the order: X = F < Cl < Br < I, if the substituent Y is fixed. It may be because the electrostatic interactions between C1 and O4 moieties decrease with the decrease of the inductive effect of X from F to I. The geometrical parameters (R(C1−O4) and R(C1−X2)) of the TSs also display better linear correlations with the substituent constants σ of Y (see Figure 2). The plots in Figure 2 show, whether X = F, Cl, Br, or I, the slopes are negative values for R(C1−O4) and positive values for R(C1−X2), respectively. That is to say, with increasing electron-withdrawing effects of Y substituents, the C1−O4 bond length decreases and the C1−X2 bond length increases, respectively. So, the stronger electron-withdrawing substituent Y in the nucleophile, the later the transition state will be produced. This point can be explained by the good linear correlations between charges Q(O4) and the substituent constants σ of Y (see Figure 3).

The main geometric feature in the TSs is the elongations of the O4−C1 and C1−X2 single bonds relative to the ion−molecule complex. Similar to that proposed by Shaik et al.,[62] we can readily define the geometric looseness (the

TABLE 3: Calculated Bond Lengths in the RC, TS, and PC for the Reactions $YC_6H_4O^- + CH_3X$ (X = F, Cl, Br, I; Y = OH, CH_3O, CH_3, H, F, Cl, CF_3) (in Å)

		RC			TS		PC	
X	Y	*R*(O4−H5)	*R*(C1−O4)	*R*(C1−X2)	*R*(C1−O4)	*R*(C1−X2)	*R*(C1−O4)	*R*(C1−X2)
F	*p*-OH	2.493	2.798	1.427	1.864	1.925	1.443	2.986
	p-CH_3O	2.504	2.793	1.427	1.860	1.929	1.444	2.955
	p-CH_3	2.511	2.802	1.426	1.858	1.933	1.445	2.953
	−H	2.520	2.807	1.426	1.853	1.939	1.445	2.946
	p-F	2.525	2.810	1.425	1.847	1.941	1.444	2.957
	p-Cl	2.530	2.814	1.424	1.833	1.954	1.446	2.949
	p-CF_3	2.557	2.835	1.422	1.809	1.979	1.449	2.925
Cl	*p*-OH	2.012	2.995	1.832	2.086	2.243	1.434	3.659
	p-CH_3O	2.018	2.992	1.833	2.081	2.248	1.435	3.569
	p-CH_3	2.025	2.997	1.833	2.078	2.252	1.436	3.591
	−H	2.033	2.995	1.832	2.073	2.258	1.437	3.570
	p-F	2.028	3.006	1.831	2.063	2.263	1.436	3.570
	p-Cl	2.048	3.019	1.830	2.046	2.278	1.438	3.564
	p-CF_3	2.086	3.045	1.829	2.013	2.308	1.440	3.527
Br	*p*-OH	1.987	2.981	1.996	2.139	2.368	1.432	3.923
	p-CH_3O	1.992	2.981	1.995	2.134	2.373	1.434	3.790
	p-CH_3	2.001	2.984	1.995	2.130	2.377	1.435	3.769
	−H	2.004	2.986	1.995	2.124	2.384	1.435	3.799
	p-F	2.006	2.993	1.994	2.112	2.390	1.436	3.761
	p-Cl	2.027	3.007	1.993	2.093	2.408	1.437	3.763
	p-CF_3	2.063	3.036	1.991	2.057	2.440	1.440	3.699
I	*p*-OH	1.952	2.991	2.184	2.203	2.522	1.432	4.120
	p-CH_3O	1.958	2.990	2.184	2.193	2.531	1.434	3.973
	p-CH_3	1.964	3.002	2.184	2.190	2.535	1.434	4.034
	−H	1.972	3.008	2.183	2.187	2.539	1.435	4.041
	p-F	1.972	3.006	2.183	2.168	2.552	1.435	4.013
	p-Cl	1.985	3.018	2.180	2.145	2.571	1.436	3.996
	p-CF_3	2.027	3.039	2.177	2.108	2.606	1.439	3.979

changing percent of bond lengths) of O4−C1 and C1−X2 single bonds in the transition state structure, % O4−C1‡ and %C1−X2‡

$$\%O4-C1^{‡} = 100[R^{‡}(O4-C1) - R^{comp}(O4-C1)]/R^{comp}(O4-C1)$$

$$\%C1-X2^{‡} = 100[R^{‡}(C1-X2) - R^{comp}(C1-X2)]/R^{comp}(C1-X2)$$

where $R^{‡}$ and R^{comp} are the bond lengths in the transition structure (**TS**) and the ion−molecule complex (**RC** or **PC**), respectively. As can be seen from Figure 4, an excellent relationship between the central barrier heights ($\Delta H^{‡}$) and the looseness of the transition state structure is found (R^2 = 0.9886), which indicates that the stretching of the cleaving bond (C1−X2) is one of the major factors determining the central barrier heights ($\Delta H^{‡}$). The other factor will be the electrostatic interactions of C1···O4 and C1···X2 moieties.

The degree of bond formation in the transition state can be predicted by the Leffler−Grunwald rate-equilibrium relationships for variations of substituents Y [eq 1].[42,63−65]

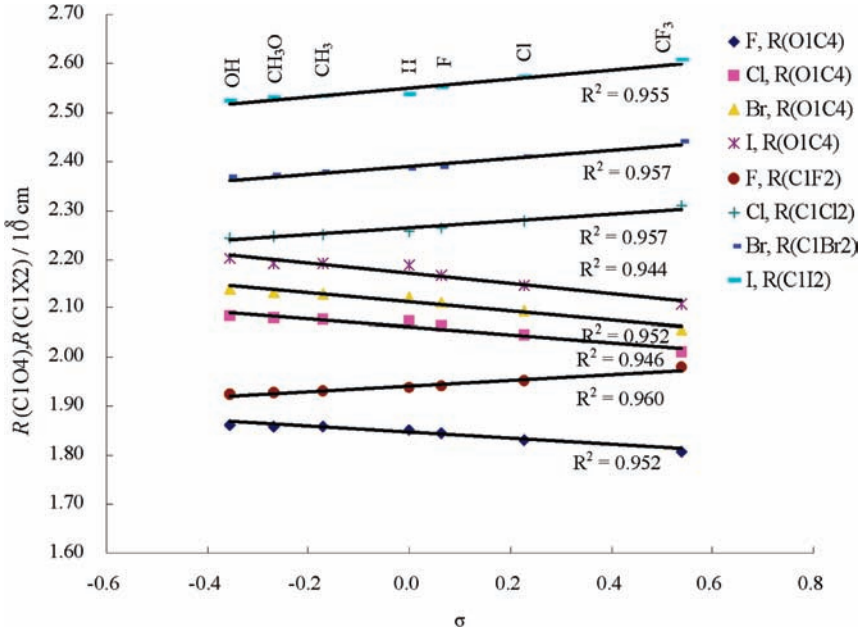

Figure 2. Plot of the calculated bond length (*R*) of TSs against the σ constants for the reactions $YC_6H_4O^- + CH_3X$ (X = F, Cl, Br, I; Y = OH, CH_3O, CH_3, H, F, Cl, CF_3). The σ constants were used from ref 61.

$$\delta\Delta G_Y^{\neq} = \alpha\delta\Delta G_Y^{o} \quad (1)$$

where $\Delta G_Y^{\ddagger}$ and ΔG_Y^{o} are the activation free energies and overall reaction free energies. This equation only applies to an elementary reaction, and the slope α is considered as a measure of the TS structure.[42,63−65] Here, we used $\Delta H^{\ddagger}$ and ΔH^{ovr} to replace $\Delta G_Y^{\ddagger}$ and ΔG_Y^{o} approximately to investigate the degree of bond formation in the transition state. The plots in Figure 5 present very good correlations ($R^2 > 0.96$) between central barrier heights and overall reaction enthalpies with slopes of 0.31 (X = F), 0.24 (X = Cl), 0.24 (X = Br), and 0.21 (X = I), respectively. Namely, the reactions have progressed 31%, 24%, 24%, and 21% in the TS for X = F, Cl, Br, and I, respectively. This is consistent with the Bell−Evans−Polanyi (BEP) principle[66] since the more endothermic reaction will lead to a later TS. The energy data in Table 1 show that the reactions for X = F are largely endothermic with value of 18.5−34.5 kcal/mol from Y = OH to CF_3, while all the reactions are exothermic for X = Cl, Br, and I (except for X = Cl, Y = CF_3).

The simplified Marcus equation[42] (eq 2) indicates that a reaction will be kinetically controlled if ΔG^{o} is constant. On the other hand, when $\delta\Delta G_0^{\ddagger}$ ($\Delta G_0^{\ddagger}$ is the intrinsic barrier) tends to be zero, the $\Delta G^{\ddagger}$ is a function only of ΔG^{o}; i.e., the reaction is thermodynamically controlled.

$$\delta\Delta G^{\ddagger} \approx \delta\Delta G_0^{\ddagger} + \alpha\delta\Delta G^{o} \quad (2)$$

Therefore, the good correlations between central barrier heights and overall reaction enthalpies shown in the plot of Figure 5 suggest that variation of the TS structure with substituents in the nucleophile is not kinetically but thermodynamically controlled, similar to the earlier results attained by Kim et al.[42]

The MP2 relative energies in Table 1 disclose the large endothermic reactions for X = F and exothermic reactions for X = Cl, Br, and I in any cases of substituent Y (except for X = Cl, Y = CF_3). In addition, the central barriers ($\Delta H^{\ddagger}$) and overall barriers (ΔH^{b}) are decreasing in the order $F > Cl > Br > I$, if the substituent Y is fixed. This may be due to the decrease of the CH_3X stability and the dissociation energy of the C−X bond in CH_3X from F to I.[67] The central barriers ($\Delta H^{\ddagger}$) or overall barriers (ΔH^{b}) also display good linear correlations with the substituent constant σ of Y (see Figures 6 and 7). The plots in Figures 6 and 7 show that the energy barriers increase with the increase of the electron-withdrawing power of substituent Y in the nucleophile. This also can be explained by the electrostatic interactions between C1 and O4 moieties, which decrease with the decrease of the negative charges Q(O4), while the overall reaction enthalpies (ΔH^{ovr}) decrease with the increase of the electron-withdrawing power of substituent Y. This is because of the enhanced stabilities of the anionic nucleophiles (**Re1**) in the initial states due to strong charge delocalization which is lost in the product, especially for the strong electron-acceptor substituents.

3.3. Nucleophilicity and Leaving-Group Ability. Nucleophilicity and leaving-group ability are important to determine the efficiency of an S_N2 reaction and will be influenced by many properties, such as the medium of the S_N2 reaction, electronegativity, size, polarizability, and others. The previous work by Olmstead and Brauman[6] revealed that the exothermicity of the reactions of nucleophile with a single substrate reflects the thermodynamic affinity of the nucleophile. Very recently, Bento and Bickelhaupt[30] used the activation strain model of chemical reactivity to study nucleophilicity and leaving-group ability in the S_N2 reactions at saturated carbon. Their results indicated that the nucleophilicity is determined by the electron-donating capability of the nucleophile, and leaving-group ability derives directly from carbon-leaving group bond strength. Here, we will discuss the nucleophilicity and leaving-group ability in the gas-phase nucleophilic substitution reactions of phenoxides with halomethanes using our MP2 energies in Table 1.

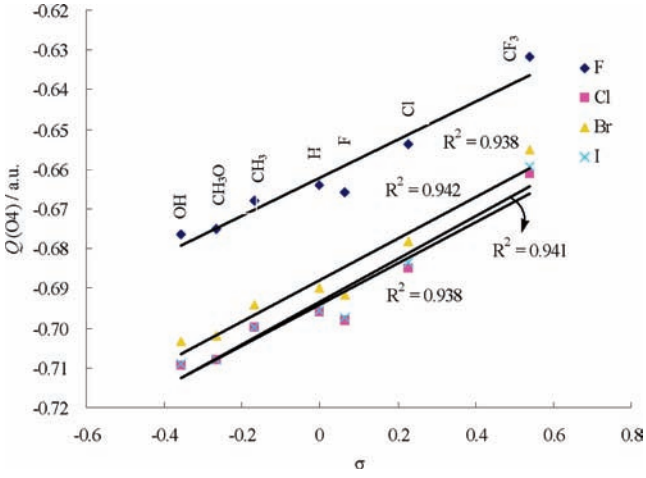

Figure 3. Plot of the calculated charges (Q) of TSs against the σ constants for the reactions $YC_6H_4O^- + CH_3X$ (X = F, Cl, Br, I; Y = OH, CH_3O, CH_3, H, F, Cl, CF_3). The σ constants were taken from ref 61 .

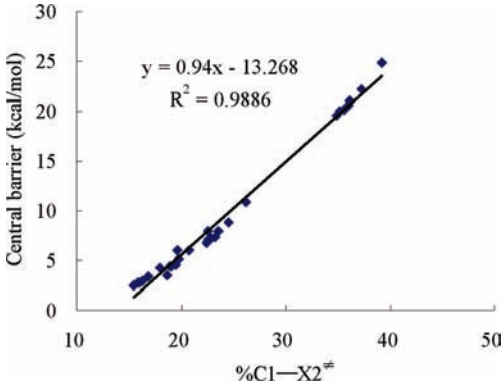

Figure 4. Plot of MP2 central barrier $\Delta H^{\ddagger}$ versus the geometric looseness of the C1−X2 bond of the TSs for the reactions $YC_6H_4O^- + CH_3X$ (X = F, Cl, Br, I; Y = OH, CH_3O, CH_3, H, F, Cl, CF_3).

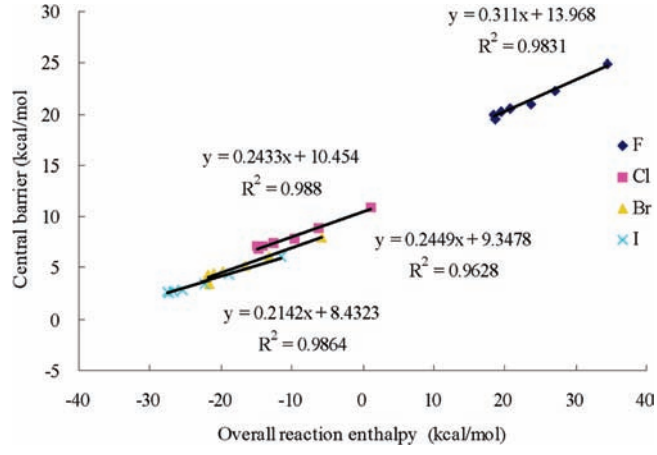

Figure 5. Plot of MP2 central barrier $\Delta H^{\ddagger}$ versus overall reaction enthalpy ΔH^{ovr} for the reactions $YC_6H_4O^- + CH_3X$ (X = F, Cl, Br, I; Y = OH, CH_3O, CH_3, H, F, Cl, CF_3).

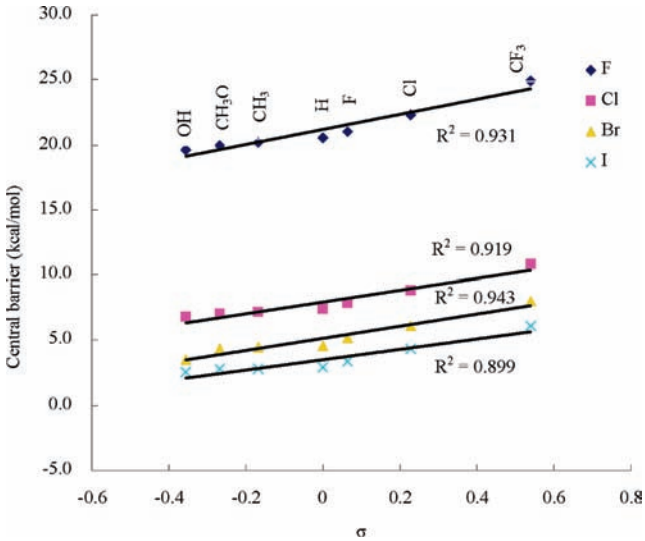

Figure 6. Plot of MP2 central barrier $\Delta H^{\ddagger}$ versus the σ constants for the reactions $YC_6H_4O^- + CH_3X$ (X = F, Cl, Br, I; Y = OH, CH_3O, CH_3, H, F, Cl, CF_3). The σ constants were taken from ref 61.

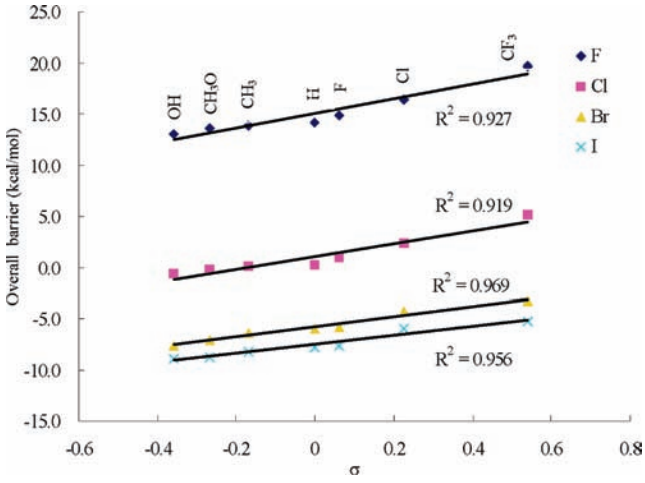

Figure 7. Plot of MP2 overall barrier ΔH^{b} versus the σ constants for the reactions $YC_6H_4O^- + CH_3X$ (X = F, Cl, Br, I; Y = OH, CH_3O, CH_3, H, F, Cl, CF_3). The σ constants were taken from ref 61.

As discussed above, whether X = F, Cl, Br, or I in the substrate, the overall reaction enthalpy change (ΔH^{ovr}) falls in the following order: Y = OH < CH_3O < CH_3 < H < F < Cl < CF_3. This overall reaction enthalpy change (ΔH^{ovr}) can be clearly related to the nucleophilicity of the nucleophile **Re1**, which follows the same trend. From a kinetic aspect study, the lower the energy barrier, the more facile for the S_N2 reaction. Thus, the barrier height can also reflect the nucleophilicity of the nucleophile. The relative energies in Table 1 show that the central barriers ($\Delta H^{\ddagger}$) and overall barriers (ΔH^{b}) increase with the increase of the electron-withdrawing power of substituent Y in the nucleophile, which are in good agreement with the overall reaction enthalpy change (ΔH^{ovr}) and show the correlation between barrier heights and overall reaction enthalpies (see Figure 5); i.e., when the energy barriers decrease, the overall reaction enthalpy change (ΔH^{ovr}) increases, and the nucleophilicity of the nucleophile increases.

Clearly, the negative charges Q(O4) in the nucleophile **Re1** decrease with the increase of the electron-withdrawing power of substituent Y in the nucleophile, following the same order as the overall reaction enthalpy change (ΔH^{ovr}). This is consistent with the result given by Bento et al.[30] that the nucleophilicity is determined by the electron-donor capability of the nucleophile.

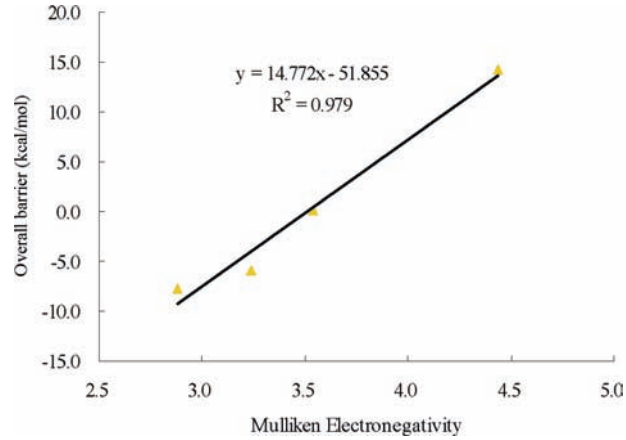

Figure 8. Plot of gas-phase MP2 overall barriers (ΔH^{b}) versus Mulliken electronegativity (in Pauling units, taken from ref 68) of the halogen atom.

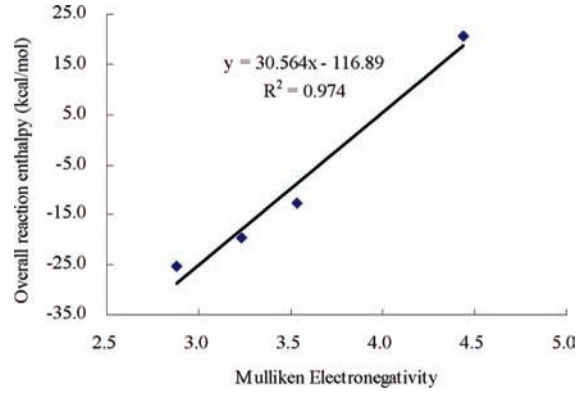

Figure 9. Plot of gas-phase MP2 overall reaction enthalpies (ΔH^{ovr}) versus Mulliken electronegativity (in Pauling units, taken from ref 68) of the halogen atom.

On the other hand, if we fix the nucleophile and change the substrate CH_3X going from X = F to I, it is found that the overall reaction enthalpy change (ΔH^{ovr}) increases in the same order. This is also related to the leaving-group ability of the halogen atom, following in the order: F < Cl < Br < I. Moreover, if the substituent Y is fixed, the central barriers ($\Delta H^{\ddagger}$) and overall barriers (ΔH^{b}) decrease in the order F < Cl < Br < I, following the same order of the overall reaction enthalpy change (ΔH^{ovr}). Therefore, the studies of the thermodynamics and kinetics lead to the same conclusion.

Interestingly, very good linear correlations (see Figures 8 and 9) have been found between overall barriers (ΔH^{b}) or overall reaction enthalpies (ΔH^{ovr}) and the Mulliken electronegativity[68] of halogen atom ($R^2 > 0.97$). Obviously, the leaving-group ability of halogen atoms increases with the decrease of its Mulliken electronegativity.

4. Conclusions

Computational investigations on the gas-phase S_N2 nucleophilic substitution reactions of phenoxides with halomethanes at the MP2/6-311+G(d,p)//B3LYP/6-311+G(d,p) level of theory lead to the following conclusions:

(1) The gas-phase energy profile is described by an asymmetrical double-well curve. The enthalpies of the reactions are largely endothermic for X = F and exothermic for X = Cl, Br, and I regardless of the substituent Y (except for X = Cl, Y = CF_3).

(2) The complexation enthalpies tend to increase from lighter halogen to the heavier halogen in CH_3X (X = F, Cl, Br, I), due to the electrostatic interactions between phenol oxygen and the hydrogen of halomethane increasing from X = F to I.

(3) With the increase of the electron-withdrawing effects of Y substituents, the C1−O4 bond length decreases and the C1−X2 bond length increases in the transition state, respectively, indicating that the stronger the electron-withdrawing substituent Y in the nucleophile, the later the transition state will be produced.

(4) The excellent relationship between the central barrier heights and the looseness of the transition state structure suggests that the stretching of the cleaving bond (C1−X2) is one of the major factors determining the central barrier heights.

(5) Leffler−Grunwald rate-equilibrium relationships predict the degree of bond formation in the transition state suggesting that the reactions have progressed 31%, 24%, 24%, and 21% in the TS for X = F, Cl, Br, and I, respectively, which is consistent with the Bell−Evans−Polanyi (BEP) principle that the more endothermic reaction will lead to a later TS.

(6) The good correlations between central barrier heights and overall reaction enthalpies reveal that variation of the TS structure with substituents in the nucleophile is not kinetically but thermodynamically controlled, as in the earlier results obtained by Kim et al.[42]

(7) Central barriers ($\Delta H^{\ddagger}$) and overall barriers (ΔH^{b}) decrease in the order F > Cl > Br > I, if the substituent Y is fixed because of the CH_3X stability, and the dissociation energy of the C−X bond in CH_3X decreases from F to I. Furthermore, the central barriers ($\Delta H^{\ddagger}$) or overall barriers (ΔH^{b}) also display good linear correlations with the substituent constants σ of Y.

(8) The nucleophilicity of the nucleophile and leaving-group ability of the halogen atom in the substrate can be estimated by investigating the thermodynamics and kinetics of the reactions. The nucleophilicity of the nucleophile is influenced by the electron-withdrawing or electron-donating power of substituents in the nucleophile. The leaving group ability of the halogen atom in the substrate is determined by its Mulliken electronegativity.

Acknowledgment. This project has been supported by the National Natural Science Foundation of China (Grant Nos. 20773089 and 20835003) and the Scientific Research Foundation for the Returned Overseas Chinese Scholars, State Education Ministry (Grant No. 20071118-18-15).

Supporting Information Available: The origin data of the figures. This material is available free of charge via the Internet at http://pubs.acs.org.

References and Notes

(1) Lowry, T. H.; Richardson, K. S. *Mechanism and Theory in Organic Chemistry*, 3rd ed.; Harper & Row: New York, 1987.

(2) Shaik, S. S.; Schlegel, H. B.; Wolfe, S. *Theoretical Aspects of Physical Organic Chemistry: The SN2 mechanism*; Wiley & Sons: New York, 1992.

(3) Williams, A. *Concerted and Bio-organic Mechanisms*, CRC Press LLC, 2000.

(4) Moylan, C. R.; Brauman, J. I. *Advances in Classical Trajectory Methods*; JAI Press Inc.: London, 1994; *Vol. 2*, p 95.

(5) Brauman, J. I.; Olmstead, W. N.; Lieder, C. A. *J. Am. Chem. Soc.* **1974**, *96*, 4030–4031.

(6) Olmstead, W. N.; Brauman, J. I. *J. Am. Chem. Soc.* **1977**, *99*, 4219–4228.

(7) Asubiojo, O. I.; Brauman, J. I. *J. Am. Chem. Soc.* **1979**, *101*, 3715–3724.

(8) Pross, A.; Shaik, S. S. *New J. Chem.* **1989**, *13*, 427–433.

(9) DePuy, C. H.; Gronert, S.; Mullin, A.; Bierbaum, V. M. *J. Am. Chem. Soc.* **1990**, *112*, 8650–8655.

(10) Wladkowski, B. D.; Lim, K. F.; Allen, W. D.; Brauman, J. I. *J. Am. Chem. Soc.* **1992**, *114*, 9136–9153.

(11) Wolfe, S.; Mitchell, D. J. *J. Am. Chem. Soc.* **1981**, *103*, 7692–7694.

(12) Li, C.; Ross, P.; Szulejko, J. E.; McMahon, T. B. *J. Am. Chem. Soc.* **1996**, *118*, 9360–9367.

(13) Wilbur, J. L.; Brauman, J. I. *J. Am. Chem. Soc.* **1994**, *116*, 9216–9221.

(14) Takeuchi, K.; Takasuka, M.; Shiba, E.; Kinoshita, T.; Okazaki, T.; Abboud, J.-L. M.; Notario, R.; Castano, O. *J. Am. Chem. Soc.* **2000**, *122*, 7351–7357.

(15) Glukhovtsev, M. N.; Bach, R. D.; Pross, A.; Radom, L. *Chem. Phys. Lett.* **1996**, *260*, 558–564.

(16) Mo, Y. R.; Gao, J. L. *J. Comput. Chem.* **2000**, *21*, 1458–1469.

(17) Parthiban, S.; de Oliveira, G.; Martin, J. M. L. *J. Phys. Chem. A* **2001**, *105*, 895–904.

(18) Gonzales, J. M.; Cox, R. S.; Braun, S. T.; Allen, W. D.; Schaefer, H. F. *J. Phys. Chem. A* **2002**, *105*, 11327–11346.

(19) Gonzales, J. M.; Pak, C.; Cox, R. S.; Allen, W. D.; Schaefer, H. F.; Csa'sza'r, A. G.; Tarcsay, G. *Chem.—Eur. J.* **2003**, *9*, 2173–2192.

(20) Gonzales, J. M.; Allen, W. D.; Schaefer, H. F. *J. Phys. Chem. A* **2005**, *109*, 10613–10628.

(21) Chabinyc, M. L.; Craig, S. L.; Regan, C. K.; Brauman, J. I. *Science* **1998**, *279*, 1882–1886.

(22) Laerdahl, J. K.; Uggerud, E. *Int. J. Mass Spectrom.* **2002**, *214*, 277–314.

(23) Uggerud, E. *J. Phys. Org. Chem.* **2006**, *19*, 461–466.

(24) Regan, C. K.; Craig, S. L.; Brauman, J. I. *Science* **2002**, *295*, 2245–2247.

(25) Vayner, G.; Houk, K. N.; Jorgensen, W. L.; Brauman, J. I. *J. Am. Chem. Soc.* **2004**, *126*, 9054–9058.

(26) Ren, Y; Yamataka, H. *Org. Lett.* **2006**, *8*, 119–121.

(27) Ren, Y; Yamataka, H. *Chem.—Eur. J.* **2007**, *13*, 677–682.

(28) Ren, Y; Yamataka, H. *J. Org. Chem.* **2007**, *72*, 5660–5667.

(29) Galabov, B.; Nikolova, V.; Wilke, J. J.; Schaefer, H. F., III; Allen, W. D. *J. Am. Chem. Soc.* **2008**, *130*, 9887–9896.

(30) Bento, A. P.; Bickelhaupt, F. M. *J. Org. Chem.* **2008**, *73*, 7290–7299.

(31) Matsson, O.; Persson, J.; Axelsson, B. S.; Langstrom, B.; Fang, Y.; Westaway, K. C. *J. Am. Chem. Soc.* **1996**, *118*, 6350–6354.

(32) Szylhabel-Godala, A.; Madhavan, S.; Rudzinski, J.; O'Leary, M. H.; Paneth, P. *J. Phys. Org. Chem.* **1996**, *9*, 35–40.

(33) Westaway, K. C.; Fang, Y.-r.; Persson, J.; Matsson, O. *J. Am. Chem. Soc.* **1998**, *120*, 3340–3344.

(34) Westaway, K. C.; Jiang, W. *Can. J. Chem.* **1999**, *77*, 879–889.

(35) Koerner, T.; Fang, Y.-r.; Westaway, K. C. *J. Am. Chem. Soc.* **2000**, *122*, 7342–7350.

(36) Westaway, K. C.; Pham, T. V.; Fang, Y.-r. *J. Am. Chem. Soc.* **1997**, *119*, 3670–3676.

(37) Wladkowski, B. D.; Wilbur, J. L.; Brauman, J. I. *J. Am. Chem. Soc.* **1994**, *116*, 2471–2480.

(38) Westaway, K. C.; Fang, Y.-r.; MacMillar, S.; Matsson, O.; Poirier, R. A.; Islam, S. M. *J. Phys. Chem. A* **2007**, *111*, 8110–8120.

(39) Ruff, F.; Farkas, Ö.; Kucsman, Á. *Eur. J. Org. Chem.* **2006**, *24*, 5570–5580.

(40) Ruff, F.; Farkas, Ö. *J. Phys. Org. Chem.* **2008**, *21*, 53–61.

(41) Ochran, R. A.; Uggerud, E. *Int. J. Mass Spectrom.* **2007**, *265*, 169–175.

(42) Kim, W. K.; Ryu, W. S.; Han, I. S.; Kim, C. K.; Lee, I. *J. Phys. Org. Chem.* **1998**, *11*, 115–124.

(43) Ando, T.; Tanabe, H.; Yamataka, H. *J. Am. Chem. Soc.* **1984**, *106*, 2084–2088.

(44) Ballistreri, F. P.; Maccarone, E.; Mamo, A. *J. Org. Chem.* **1976**, *41*, 3364–3367.

(45) Fábiána, A.; Ruffa, F.; Farkas, Ö. *J. Phys. Org. Chem.* **2008**, *21*, 988–996.

(46) Dodd, J. A.; Brauman, J. I. *J. Am. Chem. Soc.* **1984**, *106*, 5356–5357.

(47) Ruff, F.; Farkas, Ö. *J. Org. Chem.* **2006**, *71*, 3409–3416.

(48) Becke, A. D. *J. Chem. Phys.* **1993**, *98*, 5648–5652.

(49) Lee, C.; Yang, W.; Parr, R. G. *Phys. Rev. B* **1988**, *37*, 785–789.

(50) Miehlich, B.; Savin, A.; Stoll, H.; Preuss, H. *Chem. Phys. Lett.* **1989**, *157*, 200–206.

(51) Wadt, W. R.; Hay, P. J. *J. Chem. Phys.* **1985**, *82*, 284–298.

(52) Reed, A. E.; Weinstock, R. B.; Weinhold, F. *J. Chem. Phys.* **1985**, *83*, 735–746.

(53) Reed, A. E.; Curtiss, L. A.; Weinhold, F. *Chem. Rev.* **1988**, *88*, 899–926.

(54) Frisch, M. J.; Trucks, G. W.; Schlegel, H. B.; Scuseria, G. E.; Robb, M. A.; Cheeseman, J. R.; Zakrzewski, V. G.; Montgomery, J. A., Jr.; Stratmann, R. E.; Burant, J. C.; Dapprich, S.; Millam, J. M.; Daniels,

A. D.; Kudin, K. N.; Strain, M. C.; Farkas, O.; Tomasi, J.; Barone, V.; Cossi, M.; Cammi, R.; Mennucci, B.; Pomelli, C.; Adamo, C.; Clifford, S.; Ochterski, J.; Petersson, G. A.; Ayala, P. Y.; Cui, Q.; Morokuma, K.; Malick, D. K.; Rabuck, A. D.; Raghavachari, K.; Foresman, J. B.; Cioslowski, J.; Ortiz, J. V.; Stefanov, B. B.; Liu, G.; Liashenko, A.; Piskorz, P.; Komaromi, I.; Gomperts, R.; Martin, R. L.; Fox, D. J.; Keith, T.; Al-Laham, M. A.; Peng, C. Y.; Nanayakkara, A.; Gonzalez, C.; Challacombe, M.; Gill, P. M. W.; Johnson, B.; Chen, W.; Wong, M. W.; Andres, J. L.; Gonzalez, C.; Head-Gordon, M.; Replogle, E. S.; Pople, J. A. *Gaussian 03*, Revision D.01; Gaussian, Inc.: Pittsburgh, PA, 2005.

(55) Glukhovtsev, M. N.; Pross, A.; Radom, L. *J. Am. Chem. Soc.* **1995**, *117*, 2024–2032.

(56) Egawa, T.; Yamamoto, S.; Nakata, M.; Kuchitsu, K. *J. Mol. Struct.* **1987**, *156*, 213–228.

(57) Jensen, T.; Brodersen, S.; Guelachvili, G. *J. Mol. Spectrosc.* **1981**, *88*, 378–393.

(58) Graner, G. *J. Mol. Spectrosc.* **1981**, *90*, 394–438.

(59) Hannonv, M. D.; Laurie, V. W.; Kuczkowski, R. L.; Ramsav, D. A.; Lovas, F. J.; Lafferty, W. J.; Maki, A. G. *J. Phys. Chem. Ref. Data* **1979**, *8*, 619.

(60) Lide, D. R. *CRC Handbook of Chemistry and Physics*, 72nd ed.; CRC Press: Boca Raton, 1991−1992.

(61) Hansch, C.; Leo, A.; Taft, R. W. *Chem. Rev.* **1991**, *91*, 165–195.

(62) Shaik, S. S.; Schlegel, H. B.; Wolfe, S. *Theoretical Aspects of Physical Organic Chemistry. The S_N2 Mechanism*; Wiley: New York, 1992; pp 181−188.

(63) Leffler, J. E.; Grunwald, E. *Rates and Equilibria of Organic Chemistry*; Wiley: NY, 1963.

(64) Leffler, J. E. *Science* **1953**, *117*, 340–341.

(65) Pross, A. *Theoretical and Physical Principles of Organic Reactivity*; Wiley: New York, 1995; p 179.

(66) Dewar, M. J. S.; Dougherty, R. C. *The PMO Theory of Organic Chemistry*; Plenum Press: New York, 1975; p 212.

(67) Lias, S. G.; Bartmess, J. E.; Liebman, J. F.; Holmes, J. L.; Levin, R. D.; Mallard, W. G. *J. Phys. Chem. Ref. Data* **1988**, *17*, 1.

(68) Allen, L. C. *J. Am. Chem. Soc.* **1989**, *111*, 9003–9014.

JP905346E